
CHALMERS
UNIVERSITY OF TECHNOLOGY

# Sensing Assisted Robust Beamforming for mmWave Downlink Vehicle-to-Infrastructure Communications



Citation for the original published paper (version of record):
He, C., Shi, X., Wen, F. et al (2026). Sensing Assisted Robust Beamforming for mmWave Downlink Vehicle-to-Infrastructure Communications. IEEE Wireless Communications Letters, 15: 735-739.
http://dx.doi.org/10.1109/LWC.2025.3638851



(article starts on next page)

# Sensing Assisted Robust Beamforming for mmWave Downlink Vehicle-to-Infrastructure Communications

Chong He, Xiaohan Shi, Fuxi Wen, *Senior Member, IEEE* and Henk Wymeersch, *Fellow, IEEE*

***Abstract*—This paper proposes a sensing-assisted robust beamforming strategy for millimeter-wave (mmWave) vehicle-to-infrastructure communications operating in near- and far-field regions. Near-field and far-field sources classification is not required. That simplifies system design and reduces latency. Furthermore, by incorporating environmental sensing information, the proposed beamforming scheme remains robust to sensing uncertainties, ensuring reliable communication performance under highly dynamic scenarios. Simulation results validate the effectiveness of the proposed approach in terms of both spectral efficiency and robustness.**

***Index Terms*—Millimeter-wave communications, vehicular networks, near-field beamforming, far-field beamforming, robust beamforming, sensing-aided communications.**

## I. Introduction

Vehicular communication in the millimeter-wave (mmWave) band is one way to achieve high data rates for applications like connected and automated driving. It has been increasingly adopted in next-generation vehicle-to-infrastructure (V2I) communication systems [1]. In mmWave, based on the accurate channel state information (CSI), a large number of antennas and directional transmission and reception are used to achieve a sufficient link margin. With the utility of large-scale antennas, mmWave V2I communications exhibit hybrid near-field and far-field propagation characteristics [2]. The distinction between near-field and far-field channel models further complicates beamforming optimization, as conventional far-field assumptions become invalid for vehicles close to the roadside unit (RSU) [3]. A unified modeling approach is required. Furthermore, it is challenging to frequently reconfigure these large antenna arrays with minimal overhead in highly dynamic scenarios [4]. To address these challenges, sensing-assisted beamforming has emerged as a promising solution, leveraging integrated sensing and communication capabilities to assist channel estimation and enhance beam alignment [5]–[8]. Here, environmental sensing in V2I scenarios refers to the ability of the RSU to acquire vehicles ranges and directions via out-of-band information using its equipped sensing devices such as camera and LiDAR. Since the channel model depends on the distance and azimuth between the BS and UE, environmental sensing can thereby reduce the channel estimation overhead and assist in beamforming. Although learning-based beamforming methods leveraging sensing information [9], [10] demonstrate potential, they often suffer from performance loss and are sensitive to sensing inaccuracies. Robust method [11] can maintain performance under imperfect CSI, but unstructured estimation is not easy to implement in practice.

C. He, X. Shi and F. Wen are with the School of Vehicle and Mobility, Tsinghua University, Beijing, China.

H. Wymeersch is with the Department of Electrical Engineering, Chalmers University of Technology, SE-412 96 Gothenburg, Sweden.

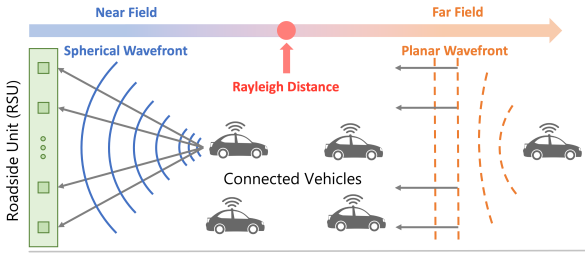


Fig. 1: Illustration of near-field and far-field V2I communications.

In this paper, we propose a sensing-assisted and unified near-field channel model robust beamforming framework for mmWave downlink V2I systems that addresses these challenges through the following key contributions: Since the far-field model can be treated as an approximation of the near-field model [12], our approach seamlessly accommodates both near-field and far-field scenarios by applying the near-field model to all UEs uniformly, simplifying beamforming design while maintaining generality. Near-field and far-field sources classification is not required. Furthermore, the proposed robust beamforming method is developed by structured modeling estimation error under sensing uncertainties and maximizing the average achievable sum-rate lower bound, outperforming the technique in [13] in terms of robustness.

## II. System Model and Problem Formulation

A downlink vehicular mmWave communication system is considered, where $M$ vehicles are randomly distributed across the far-field and near-field regions within the base station (BS) coverage (as shown in Fig.1). BS employs a full-digital uniform linear array (ULA) with $N$ antenna elements, while each vehicle is equipped with a single antenna [14]. Although this work focuses on single-antenna scenarios, future research will investigate alternative array configurations.

Let $s_m$ denotes the transmitted symbol of vehicle $m$ with $\mathbb{E}\left[|s_m|^2\right] = 1$ and $\mathbf{w}_m \in \mathbb{C}^{N\times 1}$ denotes the precoding vector for $s_m$. The received signal at the $m$th vehicle can be written as

$$y_m = \mathbf{h}_m^{\mathsf{H}}\mathbf{w}_m s_m + \sum_{i=1, i\neq m}^{M} \mathbf{h}_m^{\mathsf{H}}\mathbf{w}_i s_i + n_m, \tag{1}$$

where $\mathbf{h}_m^{\mathsf{H}} \in \mathbb{C}^{1\times N}$ denotes the channel from the BS to the $m$-th vehicle, $n_m \sim \mathcal{CN}\left(0, \sigma_n^2\right)$ represents the received noise with $\sigma_n^2$ representing the noise power.

Given that the power of NLoS paths is 10-15 dB lower than that of the LoS path [15], mmWave V2I communication mainly relies on the LoS path. Thus, we adopt the LoS channel model in this paper and the channel vector $\mathbf{h}_m$ of the $m$th vehicle can be represented as

$$\mathbf{h}_m = \alpha_m \mathbf{a}_m\left(\theta_m, r_m\right), \tag{2}$$

where $\alpha_m$ and $\mathbf{a}_m$ represent the complex-valued path gain and steering vector.

To precisely characterize the channels in cross far- and near-field scenarios, we uniformly use the near-field steering vector for all vehicles since the far-field steering vector can be regarded as an approximation of it when the distance between the BS and the vehicle exceeds the Rayleigh distance. The near-field steering vector is based on the spherical wave assumption, which can be represented as [2]

$$\mathbf{a}_m\left(\theta_m, r_m\right) = \frac{1}{\sqrt{N}}\left[e^{-jk(r_m^0 - r_m)}, \cdots, e^{-jk(r_m^{N-1} - r_m)}\right]^{\mathsf{H}}, \tag{3}$$

where $r_m$ and $\theta_m$ denote the distance and azimuth of the $m$-th vehicle from the first BS antenna, respectively. $r_m^n = \sqrt{r_m^2 + (nd)^2 - 2ndr_m \sin\theta_m}$ represents the distance from the $m$th vehicle to the $n$th antenna with $n = [0, N-1]$. Based on (1), the achievable rate of the $m$-th vehicle can be denoted as

$$R_m = \log\left(1 + \frac{|\mathbf{h}_m^{\mathsf{H}}\mathbf{w}_m|^2}{\sum_{i\neq m}^{M}|\mathbf{h}_m^{\mathsf{H}}\mathbf{w}_i|^2 + \sigma_n^2}\right), \quad m \in \mathcal{M}. \tag{4}$$

In this paper, the BS is assumed to have the capability to sense the azimuth and range of vehicles in its coverage, which can be leveraged to facilitate channel estimation. We aim to design the beamforming vectors $\{\mathbf{w}_m\}_{m\in\mathcal{M}}$ based on the estimated CSI that maximizes the achievable sum-rate with a given transmit power constraint $P_{\max}$. The optimization problem can be written as

$$\begin{aligned} &\max_{\{\mathbf{w}_m\}} \sum_{m=1}^{M} R_m \\ &\text{s.t.} \sum_{m=1}^{M} \|\mathbf{w}_m\|^2 \le P_{\max}, \quad m \in \mathcal{M}. \end{aligned} \tag{5}$$

For the general case of $M > 1$, problem (5) is non-convex and intractable to solve. One way to solve the above problem is to transform it into the weighted sum mean-squared error (MSE) minimization [16], [17]. Considering the nominal receive filter $u_m^*$ at the $m$th vehicle as an auxiliary variable (where $\hat{s}_m = u_m^* y_m$), the MSE of the received signal of the $m$th vehicle can be represented as

$$\begin{aligned} e_m &= \mathbb{E}\left[(\hat{s}_m - s_m)(\hat{s}_m - s_m)^*\right] \\ &= 1 - u_m^*\mathbf{h}_m^{\mathsf{H}}\mathbf{w}_m - u_m\mathbf{w}_m^{\mathsf{H}}\mathbf{h}_m \\ &\quad + \sum_{i=1}^{M}|u_m\mathbf{h}_m^{\mathsf{H}}\mathbf{w}_i|^2 + |u_m|^2\sigma_n^2. \end{aligned} \tag{6}$$

The receive filter that minimizes $e_m$ can be calculated as

$$u_m^{\text{MMSE}} = \frac{\mathbf{h}_m^{\mathsf{H}}\mathbf{w}_m}{\sum_{i=1}^{M}|\mathbf{h}_m^{\mathsf{H}}\mathbf{w}_i|^2 + \sigma_n^2}. \tag{7}$$

Substituting (7) into (6), the MMSE can be obtained as

$$e_m^{\text{MMSE}} = \left(1 + \frac{|\mathbf{h}_m^{\mathsf{H}}\mathbf{w}_m|^2}{\sum_{i\neq m}^{M}|\mathbf{h}_m^{\mathsf{H}}\mathbf{w}_i|^2 + \sigma_n^2}\right)^{-1}. \tag{8}$$

It is noted that the achievable rate $R_m$ can be expressed as $R_m = -\log_2\left(e_m^{\text{MMSE}}\right)$, which illustrates the relation between achievable rate and MSE. The following Remark can be derived by further leveraging the relationship between sum-rate maximization and weighted sum-MSE minimization [16].

*Remark: Problem (5) has the same global optimal solution as the following problem*

$$\begin{aligned} &\min_{\{\mathbf{w}_m, u_m, w_m\}} \sum_{m=1}^{M} w_m e_m(u_m, \{\mathbf{w}_m\}) - \log(w_m) \\ &\text{s.t.} \sum_{m=1}^{M} \|\mathbf{w}_m\|^2 \le P_{\max}, \quad m \in \mathcal{M}, \end{aligned} \tag{9}$$

*where $w_m$ denotes the MSE-weight and $e_m(u_m, \{\mathbf{w}_m\})$ is given by (6).*

The problem (9) is convex for each optimization variable when the remaining two are fixed. Hence, the block coordinate descent method can be applied to solve (9), resulting in the procedure summarized as Algorithm 1 [13].

**Algorithm 1:** Alternating Optimization Method

**Input:** $\{\mathbf{h}_m\}$, $\sigma_n$, $P_{max}$

**Initialize:** $n = 0$; $\mathbf{w}_m^0 = \sqrt{\frac{P_{max}}{M}}\frac{\mathbf{h_m}}{\|\mathbf{h_m}\|}, \forall m$;

**repeat**

Update $n = n + 1$;

Update $u_m^n = \frac{\mathbf{h}_m^{\mathsf{H}}\mathbf{w}_m^{n-1}}{\sum_{i=1}^{M}|\mathbf{h}_m^{\mathsf{H}}\mathbf{w}_i^{n-1}|^2 + \sigma_n^2}, \forall m$;

Update $w_m^n = \left(e_m(u_m^n, \{\mathbf{w}_m^{n-1}\})\right)^{-1}, \forall m$;

Update $\mathbf{w}_m^n =$

$u_m^n w_m^n \left(\sum_{i=1}^{M} w_i^n |u_i^n|^2 \mathbf{h}_i\mathbf{h}_i^{\mathsf{H}} + \lambda\mathbf{I}_N\right)^{-1}\mathbf{h}_m, \forall m$;

**until** *convergence of* $\{\mathbf{w}_m\}$;

**Output:** $\{\mathbf{w}_m\}$

In each iteration, the algorithm first calculates the receive filters $\{u_m\}$ that minimize the MSE. Then, the MSE-weights $\{w_m\}$ are set to be $w_m = e_m^{-1}, \forall m$, leading to the same gradient of the cost function of the sum-rate maximization (5) and the weighted sum-MSE minimization (9) for a given set $\{\mathbf{w}_m\}$ [17]. Afterward, the precoding vectors $\{\mathbf{w}_m\}$ are updated to minimize the cost function of (9) with fixed $\{u_m\}$ and $\{\mathbf{w}_m\}$ under transmit power constraint.

## III. Proposed Robust Beamforming Method

Acknowledge that environmental sensing is susceptible to inaccuracies, we assume that there exist a direction estimation error $\triangle\theta_m$ and a distance estimation error $\triangle r_m$ for the $m$th vehicle, with both having zero mean and variances of $\sigma_{r_m}^2$ and $\sigma_{\theta_m}^2$, respectively. The actual steering vector expressed using the presumed direction $\hat{\theta}_m$, distance $\hat{r}_m$, and estimation error $\triangle\theta_m$, $\triangle r_m$ can be written as

$$\mathbf{a}_m\left(\theta_m, r_m\right) = \mathbf{a}_m\left(\hat{\theta}_m + \triangle\theta_m, \hat{r}_m + \triangle r_m\right). \tag{10}$$

Using the first-order Taylor expansion, the $n$th element in (10) can be expressed as

$$e^{jk(r_m^n-r_m)} \approx e^{jk(\hat{r}_m^n-\hat{r}_m)}\times \left[1+jk\left(\frac{\partial \hat{r}_m^n}{\partial \hat{r}_m}-1\right)\triangle r_m + jk\frac{\partial \hat{r}_m^n}{\partial \hat{\theta}_m}\triangle\theta_m\right], \tag{11}$$

where $\hat{r}_m^n = \sqrt{\hat{r}_m^2+(nd)^2-2nd\hat{r}_m\sin\hat{\theta}_m}$, $\partial\hat{r}_m^n/\partial\hat{r}_m = (\hat{r}_m - nd\sin\hat{\theta})/\hat{r}_m^n$ and $\partial\hat{r}_m^n/\partial\hat{\theta}_m = -\hat{r}_m nd\cos\hat{\theta}_m/\hat{r}_m^n$. We define the error for the $n$th element $\varepsilon_m^n$ and the error vector $\mathbf{v}_m$ of the steering vector $\mathbf{a}_m$ as

$$\begin{aligned}\varepsilon_m^i &= jke^{jk(\hat{r}_m^n-\hat{r}_m)}\left[\left(\frac{\partial\hat{r}_m^n}{\partial\hat{r}_m}-1\right)\triangle r_m + \frac{\partial\hat{r}_m^n}{\partial\hat{\theta}_m}\triangle\theta_m\right]\\ \mathbf{v}_m &= \frac{1}{\sqrt{N}}\begin{bmatrix}\varepsilon_m^0 & \varepsilon_m^1 & \cdots & \varepsilon_m^{N-1}\end{bmatrix}^T.\end{aligned} \tag{12}$$

Thus, the error of the steering vector caused by estimation errors in direction and distance can be expressed as an additive random deviation

$$\mathbf{a}_m(\theta_m, r_m) = \mathbf{a}_m(\hat{\theta}_m, \hat{r}_m) + \mathbf{v}_m. \tag{13}$$

We use $\hat{\mathbf{h}}_m = \hat{\alpha}_m\mathbf{a}_m(\hat{\theta}_m,\hat{r}_m)$ to denote the presumed channel model. Since the normalized path gain is insensitive to small-scale changes in the relative position between the RSU and the vehicle when $r > 1.2D$ [18], we neglect the path gain estimation error induced by $\triangle r$ and $\triangle\theta$. Then the received signal at the $m$th vehicle with receive filter $u_m^*$ is

$$\hat{s}_m = u_m^*\Big[\Big(\hat{\mathbf{h}}_m + \hat{\alpha}_m\mathbf{v}_m\Big)^{\mathsf{H}}\sum_{i=1}^{M}\mathbf{w}_i s_i + n_m\Big]. \tag{14}$$

With random channel error $\hat{\alpha}_m\mathbf{e}_m$, the average MSE of the received signal of $m$th vehicle can be derived as

$$\begin{aligned}\bar{e}_m =& \mathbb{E}(e_m) = \mathbb{E}\Big[(\hat{s}_m - s_m)(\hat{s}_m - s_m)^*\Big]\\ =& 1 - u_m^*\hat{\mathbf{h}}_m^{\mathsf{H}}\mathbf{w}_m - u_m\mathbf{w}_m^{\mathsf{H}}\hat{\mathbf{h}}_m + \sum_{i=1}^{M}|u_m\hat{\mathbf{h}}_m^{\mathsf{H}}\mathbf{w}_i|^2\\ &+ |u_m\hat{\alpha}_m|^2\sum_{i=1}^{M}\mathbf{w}_i^{\mathsf{H}}\mathbf{C}_m\mathbf{w}_i + |u_m|^2\sigma_n^2,\end{aligned} \tag{15}$$

where $\mathbf{C}_m$ is the covariance matrix of $\mathbf{v}_m$, whose $i$-$j$-th element is

$$(\mathbf{C}_m)_{ij} = \frac{1}{N}\mathbb{E}\left[\varepsilon_m^i(\varepsilon_m^j)^*\right] = \frac{1}{N}k^2e^{jk(\hat{r}_m^i-\hat{r}_m^j)}\times \left[\left(\frac{\partial\hat{r}_m^i}{\partial\hat{r}_m}-1\right)\left(\frac{\partial\hat{r}_m^j}{\partial\hat{r}_m}-1\right)\sigma_{r_m}^2 + \left(\frac{\partial\hat{r}_m^i}{\partial\hat{\theta}_m}\right)\left(\frac{\partial\hat{r}_m^j}{\partial\hat{\theta}_m}\right)\sigma_{\theta_m}^2\right]. \tag{16}$$

Refering to [19], the expected achievable rate of $m$th vehicle $\bar{R}_m$ can be lower bounded by

$$\begin{aligned}\bar{R}_m &= \mathbb{E}\left[-\log_2\left(e_m^{\text{MMSE}}\right)\right]\\ &\geq -\log_2\left[\mathbb{E}\left(e_m^{\text{MMSE}}\right)\right] = -\log_2\left(\bar{e}_m^{\text{MMSE}}\right).\end{aligned} \tag{17}$$

We define the expected achievable rate lower bound $\bar{R}_m^{LB}$ as $\bar{R}_m^{\text{LB}} = -\log_2\left(\bar{e}_m^{\text{MMSE}}\right)$. With estimation error, our target is to maximize the sum of the expected achievable rate lower bound

$$\begin{aligned}&\max_{\{\mathbf{w}_m\}}\sum_{m=1}^{M}\bar{R}_m^{\text{LB}}\\ &\text{s.t.}\sum_{m=1}^{M}\|\mathbf{w}_m\|^2 \leq P_{\max},\quad m\in\mathcal{M}.\end{aligned} \tag{18}$$

Based on the previous derivations in Sec.III, (18) can be solved by implementing a similar procedure to Algorithm 1. In this case, the updated receive filters $\{u_m\}$ minimize the average MSE $\bar{e}_m$, which can be written as

$$u_m = \frac{\hat{\mathbf{h}}_m^{\mathsf{H}}\mathbf{w}_m}{\sum_{i=1}^{M}|\hat{\mathbf{h}}_m^{\mathsf{H}}\mathbf{w}_i|^2 + |\hat{\alpha}_m|^2\sum_{i=1}^{M}\mathbf{w}_i^{\mathsf{H}}\mathbf{C}_m\mathbf{w}_i + \sigma_n^2}. \tag{19}$$

The updated weights $\{w_m\}$ can be expressed as $w_m = (\bar{e}_m)^{-1}$, where $\bar{e}_m$ is given by (15). The updated precode vectors $\{\mathbf{w}_m\}$ minimize the cost function of (9) after replacing $e_m$ with $\bar{e}_m$, leading to the following result:

$$\mathbf{w}_m = u_m w_m\Big[\sum_{i=1}^{M}w_i|u_i|^2(\hat{\mathbf{h}}_i\hat{\mathbf{h}}_i^{\mathsf{H}} + |\hat{\alpha}_i|^2\mathbf{C}_i) + \lambda\mathbf{I}_N\Big]^{-1}\hat{\mathbf{h}}_m. \tag{20}$$

Hence, the robust beamforming algorithm considering random estimation errors of the vehicles' distance and direction can be summarized as follows:

**Algorithm 2:** Robust Alternating Optimization Method

**Input:** $\{\hat{\mathbf{h}}_m\}$, $\sigma_n$, $P_{max}$, $\{\sigma_{r_m}\}$, $\{\sigma_{\theta_m}\}$
**Initialize:** $n=0$; $\mathbf{w}_m^0 = \sqrt{\frac{P_{max}}{M}}\frac{\mathbf{h_m}}{\|\mathbf{h_m}\|}, \forall m$;
**repeat**
  Update $n = n+1$;
  Update $u_m^n|\{\mathbf{w}_m^{n-1}\}$ by (19), $\forall m$;
  Update $w_m^n = \left(\bar{e}_m(u_m^n, \{\mathbf{w}_m^{n-1}\})\right)^{-1}, \forall m$;
  Update $\mathbf{w}_m^n|\{u_m^n\}, \{w_m^n\}$ by (20), $\forall m$;
**until** *convergence of* $\{\mathbf{w}_m\}$;
**Output:** $\{\mathbf{w}_m\}$

### A. Computational Complexity

The computational complexity of the algorithm mainly depends on the number of antenna elements $N$ and the number of vehicles $M$. As for Algorithm 1, the computational complexities of calculating $u_m^n$, $w_m^n$ in each iteration are both $\mathcal{O}(MN)$, while that of calculating $\mathbf{w}_m^n$ is $\mathcal{O}\left(MN^2+N^3\right)$. Therefore, the total complexity of computing $\{u_m^n\}$, $\{w_m^n\}$ and $\{\mathbf{w}_m^n\}$for $\forall m\in\mathcal{M}$ in one iteration is $\mathcal{O}\left(M^2N+M^2N^2+MN^3\right) = \mathcal{O}\left(M^2N^2+MN^3\right)$.

As for Algorithm 2, an additional term $\sum_{i=1}^{M}\mathbf{w}_i^{\mathsf{H}}\mathbf{C}_m\mathbf{w}_i$ needs to be computed. Note that $\mathbf{C}_m$ can be written as $\mathbf{C}_m = \mathbf{C}_{m_\theta} + \mathbf{C}_{m_r} = \mathbf{c}_{m_\theta}\mathbf{c}_{m_\theta}^H + \mathbf{c}_{m_r}\mathbf{c}_{m_r}^H$, where $(\mathbf{c}_{m_r})_i = \frac{1}{\sqrt{N}}ke^{jk\hat{r}_m^i}\left(\partial\hat{r}_m^i/\partial\hat{r}_m - 1\right)\sigma_{r_m}$ and $(\mathbf{c}_{m_\theta})_i = \frac{1}{\sqrt{N}}ke^{jk\hat{r}_m^i}\left(\partial\hat{r}_m^i/\partial\hat{\theta}_m\right)\sigma_{\theta_m}$. Thus, $\sum_{i=1}^{M}\mathbf{w}_i^{\mathsf{H}}\mathbf{C}_m\mathbf{w}_i$ is equivalent to $\sum_{i=1}^{M}|\mathbf{c}_{m_\theta}^{\mathsf{H}}\mathbf{w}_i|^2 + \sum_{i=1}^{M}|\mathbf{c}_{m_r}^{\mathsf{H}}\mathbf{w}_i|^2$, and the latter can reduce the computaional complexity from $\mathcal{O}\left(MN^2\right)$ to $\mathcal{O}(MN)$. In this case, the computational complexities

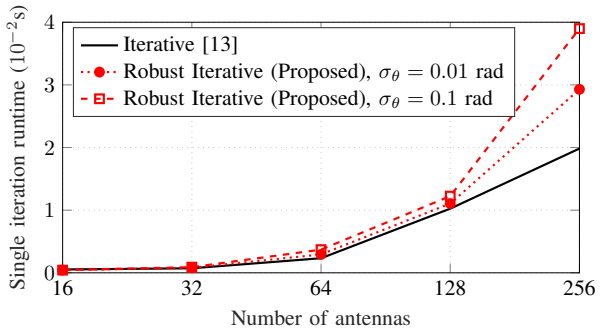


Fig. 2: Single iteration runtime comparison.

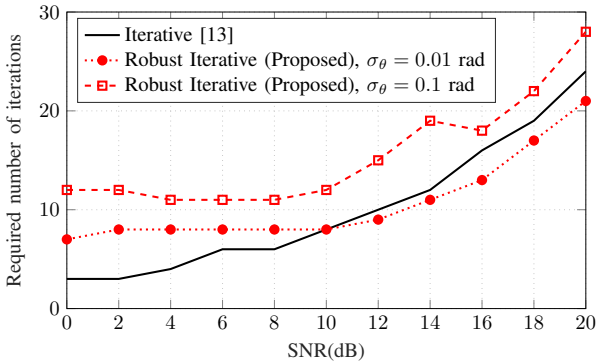


Fig. 3: Required number of iterations until convergence against SNR, without distance errors.

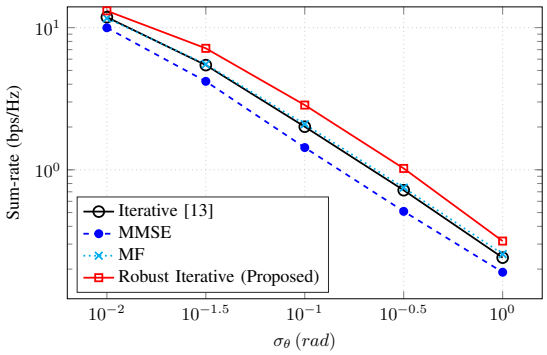


(a) Sum-rate vs different direction errors, without distance errors

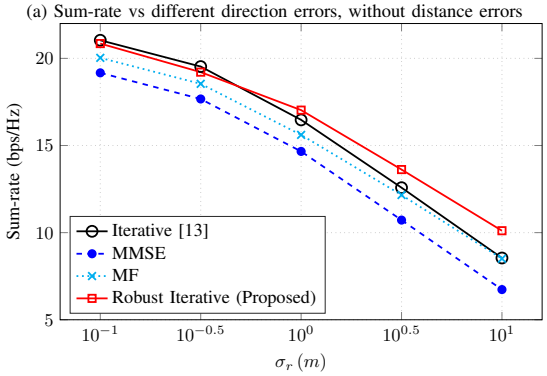


(b) Sum-rate vs different distance errors, without direction errors

Fig. 4: Improvement of the robust algorithm in sum-rate under different estimation error distributions.

of calculating $u_m^n$, $w_m^n$ and $\mathbf{w}_m^n$ in algorithm 2 are also $\mathcal{O}(MN)$ and $\mathcal{O}\left(MN^2 + N^3\right)$, resulting in the computational complexity of Algorithm 2 being equal to that of Algorithm 1.

Fig 2 compares the single iteration runtimes of the two algorithms under different numbers of antennas and sensing errors, and the numerical results are basically consistent with the complexity analysis. Although the runtime of the proposed algorithm will slight increase with the growth of $\sigma_\theta$ because of the need to calculate additional terms, the improvement in sum-rate of it compared to the baseline will also become larger accordingly.

### *B. Convergence Speed and Stability*

Figure 3 is plotted to evaluate the convergence speed of the proposed algorithm, which illustrates the required number of iterations until convergence for the algorithms under different SNR when $\sigma_\theta = 0.01$ rad and $\sigma_\theta = 0.1$ rad. The convergence criterion is set to $\sum_m \|\mathbf{w}_m^{n+1} - \mathbf{w}_m^n\| < 10^{-3}$.

The explanation for the increase in the number of iterations as the SNR rises is as follows: We initialize $\mathbf{w}_m^0$ using the results of the matched filter algorithm. MF algorithm does not account for the interference signals in multi-user scenarios, while the result of iterative algorithms $\mathbf{w}_m^{\text{opt}}$ aims to potentially reduce inter-user interference by optimizing the sum-rate. As the interference-to-noise ratio (INR) induced by the initial $\mathbf{w}_m^0$ grows with increasing SNR, the distance $\|\mathbf{w}_m^{\text{opt}} - \mathbf{w}_m^0\|_2$ between $\mathbf{w}_m^{\text{opt}}$ and $\mathbf{w}_m^0$ expands at the same time, resulting in more iterations.

For the convergence stability, since the optimization problem obtained by replacing $e_m$ with $\bar{e}_m$ in equation (9) can be regarded as the equivalent optimization problem of the proposed iterative algorithm, the cost function of this problem is still convex with respect to each of the optimization variables $\{\mathbf{w}_m, u_m, w_m\}$. Therefore, by updating one variable at a time while keeping the other two variables fixed, the proposed algorithm is guaranteed to converge to a stationary point.

## IV. Numerical Results

In this section, we evaluate the performance of the proposed robust beamforming method in Algorithm 2. We consider a V2I communication system consisting of one base station equipped with a 256-antenna ULA and $M = 4$ single-antenna vehicles. The wavelength is $\lambda$ = 0.005 meters, corresponding to a frequency of 60 GHz. The antenna spacing is set to be $d = \lambda/2$. The path gain $\alpha_m$, angle $\theta_m$ and distance $r_m$ of each vehicle are generated as following: $\alpha_m \sim \mathcal{CN}(0,1)$, $\theta_m \sim \mathcal{U}(-1,1)$, and $r_m \sim \mathcal{U}(20,200)$. The SNR is set as $P_{\max}/\sigma_n^2 = 20$dB. For the imperfect CSI, we assume that the estimation errors of distance $\triangle r_m$ and direction $\triangle\theta_m$ for each vehicle are normally distributed with variances $\sigma_r^2$ and $\sigma_\theta^2$, respectively. With the imperfect CSI, the performance of the proposed method is compared with that of the iterative algorithm [13], as well as the classical matched filter (MF) and minimum mean square error (MMSE) methods. The results are averaged over 5,000 channel simulations.

Considering that the sensing accuracies of different V2I systems vary, we plot the performance of the proposed method

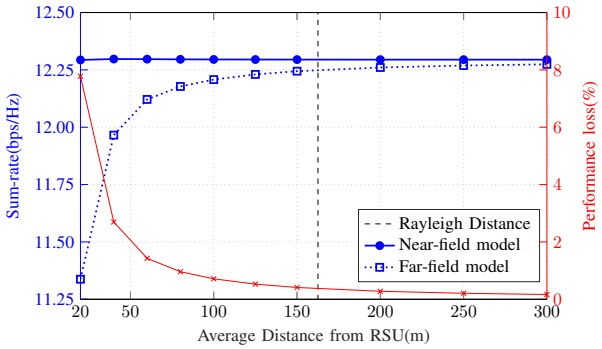


Fig. 5: The performance of using far-field and near-field steering vectors under different average distances when $\sigma_\theta$ = 0.02 rad, without distance errors.

and the iterative algorithm against $\sigma_\theta$ and $\sigma_r$ in Fig. 4. It is noted in Fig. 4a that the proposed method achieves higher sum-rates than the iterative algorithm [13] at every $\sigma_\theta$, which validates the effectiveness and robustness of the proposed method against angular sensing errors. Fig. 4b shows that when $\sigma_r$ exceeds a certain threshold, the proposed method outperforms the iterative algorithm, demonstrating its ability to compensate for distance errors. Nevertheless, when $\sigma_r$ is low, the performance of the proposed method is inferior to that of the iterative algorithm. The reason is that the performance of the iterative algorithm exhibits lower sensitivity to distance errors than to angular errors. Specifically, in the scenario where $\sigma_r$ is small, the degree of steering vector mismatch induced by distance errors remains relatively low, enabling the iterative algorithm to maintain a satisfactory performance level, while the proposed method exhibits performance degradation due to factors such as truncation errors introduced in (11). As $\sigma_r$ increases gradually, the effect of the proposed method in compensating for the steering vector mismatch becomes increasingly evident.

Fig. 5 demonstrates the necessity of using the near-field model in the cross near- and far-field scenario. The average distance between the vehicles and the RSU is used to reflect the distribution of vehicles in the near-field and far-field regions. When the average distance exceeds the Rayleigh distance, the performance of assuming the near- and far-field model is close. As the average distance decreases, the near-field path components in the system become dominant. In such cases, the far-field model fails to match the near-field channel features, resulting in significant performance loss.

## V. Conclusion

We proposed a sensing-assisted, unified near-field channel model-based beamforming framework for mmWave downlink V2I systems. The proposed approach eliminates the requirements for near-field and far-field source classification, simplifying beamforming design while maintaining generality. We also addressed the impact of environmental sensing inaccuracies by modeling range and angle estimation errors and formulated a robust beamforming optimization problem to maximize the achievable sum-rate under imperfect CSI.

## References

[1] A. Ali, N. Gonzalez-Prelcic, R. W. Heath, and A. Ghosh, "Leveraging sensing at the infrastructure for mmWave communication," *IEEE Communications Magazine*, vol. 58, no. 7, pp. 84–89, 2020.

[2] X. Wei and L. Dai, "Channel estimation for extremely large-scale massive MIMO: Far-field, near-field, or hybrid-field?" *IEEE Communications Letters*, vol. 26, no. 1, pp. 177–181, 2022.

[3] A. Guerra, F. Guidi, D. Dardari, and P. M. Djurić, "Near-field tracking with large antenna arrays: Fundamental limits and practical algorithms," *IEEE Transactions on Signal Processing*, vol. 69, pp. 5723–5738, 2021.

[4] M. Giordani, M. Polese, A. Roy, D. Castor, and M. Zorzi, "A tutorial on beam management for 3GPP NR at mmWave frequencies," *IEEE Communications Surveys & Tutorials*, vol. 21, no. 1, pp. 173–196, 2019.

[5] Y. Wang, A. Klautau, M. Ribero, A. C. K. Soong, and R. W. Heath, "Mmwave vehicular beam selection with situational awareness using machine learning," *IEEE Access*, vol. 7, pp. 87 479–87 493, 2019.

[6] R. Benelmir, S. Bitam, S. Fowler, and A. Mellouk, "A novel mmWave beam alignment approach for beyond 5G autonomous vehicle networks," *IEEE Transactions on Vehicular Technology*, vol. 73, no. 2, pp. 1597–1610, 2024.

[7] W. Yuan, F. Liu, C. Masouros, J. Yuan, D. W. K. Ng, and N. González-Prelcic, "Bayesian predictive beamforming for vehicular networks: A low-overhead joint radar-communication approach," *IEEE Transactions on Wireless Communications*, vol. 20, no. 3, pp. 1442–1456, 2021.

[8] F. Pedraza and G. Caire, "Sensing-assisted beam tracking for mmwave V2I communications with analog, hybrid, and digital antenna architectures," *IEEE Transactions on Wireless Communications*, vol. 24, no. 1, pp. 447–461, 2025.

[9] K. Patel and R. W. Heath, "Harnessing multimodal sensing for multi-user beamforming in mmwave systems," *IEEE Transactions on Wireless Communications*, vol. 23, no. 12, pp. 18 725–18 739, 2024.

[10] J. Xie, C. Luo, and Y. Luo, "Cross near- and far-field beamforming for wideband multi-user terahertz communications," *IEEE Communications Letters*, vol. 28, no. 10, pp. 2397–2401, 2024.

[11] R. Fritzsche and G. P. Fettweis, "Robust sum rate maximization in the multi-cell mu-mimo downlink," in *2013 IEEE Wireless Communications and Networking Conference (WCNC)*, 2013, pp. 3180–3184.

[12] M. Cui, Z. Wu, Y. Lu, X. Wei, and L. Dai, "Near-field MIMO communications for 6G: Fundamentals, challenges, potentials, and future directions," *IEEE Communications Magazine*, vol. 61, no. 1, pp. 40–46, 2023.

[13] H. Zhang, N. Shlezinger, F. Guidi, D. Dardari, M. F. Imani, and Y. C. Eldar, "Beam focusing for near-field multiuser MIMO communications," *IEEE Transactions on Wireless Communications*, vol. 21, no. 9, pp. 7476–7490, 2022.

[14] L. Jiang and H. Jafarkhani, "Multi-user analog beamforming in millimeter wave MIMO systems based on path angle information," *IEEE Transactions on Wireless Communications*, vol. 18, no. 1, pp. 608–619, 2019.

[15] S. Ju, Y. Xing, O. Kanhere, and T. S. Rappaport, "Millimeter wave and sub-terahertz spatial statistical channel model for an indoor office building," *IEEE Journal on Selected Areas in Communications*, vol. 39, no. 6, pp. 1561–1575, 2021.

[16] Q. Shi, M. Razaviyayn, Z.-Q. Luo, and C. He, "An iteratively weighted MMSE approach to distributed sum-utility maximization for a MIMO interfering broadcast channel," *IEEE Transactions on Signal Processing*, vol. 59, no. 9, pp. 4331–4340, 2011.

[17] S. S. Christensen, R. Agarwal, E. De Carvalho, and J. M. Cioffi, "Weighted sum-rate maximization using weighted MMSE for MIMO-BC beamforming design," *IEEE Transactions on Wireless Communications*, vol. 7, no. 12, pp. 4792–4799, 2008.

[18] E. Bjornson, T. Demir, and L. Sanguinetti, "A primer on near-field beamforming for arrays and reconfigurable intelligent surfaces," in *55th Asilomar Conference on Signals, Systems, and Computers*, 2021, pp. 105–112.

[19] F. Negro, I. Ghauri, and D. T. Slock, "Sum rate maximization in the noisy MIMO interfering broadcast channel with partial CSIT via the expected weighted MSE," in *International Symposium on Wireless Communication Systems*, 2012, pp. 576–580.